



Threshold Analysis of Wavelet Based Fingerprint Feature Extraction Methods on Multiple Impression Dataset

P. Amoako-Yirenkyi^{1,2*}, N. K. Frempong^{1,2}, J. K. Appati¹,
J. B. Hafron-Acquah³ and I. K. Dontwi^{1,2}

¹Department of Mathematics, Kwame Nkrumah University of Science and Technology, Ghana.

²Scientific and Technical Computing, National Institute for Mathematical Sciences, Ghana.

³Department of Computer Science, Kwame Nkrumah University of Science and Technology, Ghana.

Article Information

DOI: 10.9734/BJMCS/2015/13000

Editor(s):

(1) Victor Carvalho, Polytechnic Institute of Cvado and Ave, Portuguese Catholic University and Lusiada University, Portugal.

Reviewers:

(1) Anonymous, Product and Development Cell, Tech Nivarana, India.

(2) Anonymous, Department of Computer Engineering, National Institute of Technology-Kurukshetra, India.

(3) Seifedine Kadry, Faculty of General Education, American University of the Middle East, Kuwait.

(4) Iwasokun G. B, Tshwane University of Technology, Pretoria, South Africa.

Complete Peer review History:

<http://www.sciencedomain.org/review-history.php?iid=727&id=6&aid=6883>

Original Research Article

Received: 27 July 2014; Accepted: 25 September 2014; Published: 11 November 2014

Abstract

In recent years, fingerprint recognition has been moving through series of evolutions with the intent to decrease the False Acceptance Rate (FAR) and the False Rejection Rate (FRR) in order to achieve minimum Equal Error Rate (EER) while increasing recognition rate. In practical cases, fingerprint images stored in fingerprint databases may have come from scanners with different specifications under variant environmental conditions which may produce different or multiple impressions and backgrounds. The choice of what single and acceptable threshold value to use in order to characterize fingerprint features in images for recognition is therefore crucial in establishing a minimal EER. In this paper, we investigate and analyze the effect of several threshold values on EER when several families of wavelets based methods for feature extraction are applied on multiple impression datasets (Fingerprint Verification Competition-FVC2004). After conducting several threshold analysis on extracted features from multiple impression dataset, the results show

*Corresponding author: E-mail: amoakoyirenkyi@knust.edu.gh

that among the closely related wavelets families studied, the Reversed Bi-Orthogonal type 3.1 wavelet, analyzed with threshold value of 27 significantly topped with EER of 4.2% and a recognition rate of 95%. It however performed quite poorly outside of the threshold value indicating the importance of threshold analysis on datasets used for recognition.

Keywords: EER; FAR; FRR; Fingerprint recognition; Performance Rate; Recognition; Threshold Analysis; Wavelets

2010 Mathematics Subject Classification: 53C25; 83C05; 57N16

1 Introduction

Among the various behavioural and physiological characteristics identified as a biometric for humans, the use of a persons iris, gait, voice, face, fingerprint and sometimes palm to classify, identify and possibly recognize that person based on existing database is currently not in doubt [1,2,3,4,5]. As the number of usage level and use cases increases, the number of practical scenarios that prevents existing and otherwise good methods to perform poorly also increases. In the last decade, the use of various biometric technologies [6,7,8] has expanded from its original and early use of forensics and security authentication to election and voting processes, driver licensing and other social service programs [9]. Fingerprint which is basically traces of an impression left by the friction ridges of any part of a human finger [10] is one of the most widely used biometric for such use cases.

After years of using particularly, fingerprint as a biometric, a complete and accurate characterization and recognition of a person using fingerprint is yet to be realized. A fundamental cause of poor characterization or feature extraction depends heavily on available fingerprint sensor technology used to scan the fingerprint image. The way a persons finger is scanned may create different impressions making it difficult to use one type of feature to characterize and identify a person by his finger leading to poor recognition rate. Again, people with no or few minutia points [11] such as surgeons who often wash their hands with strong detergents as well as people with special skin conditions [12] will have low recognition rate since not all the minutia points can be extracted fully making it a limiting factor for security response when minutia based algorithm is used. Unfortunately extraction of fingerprint features while avoiding different impressions made due to fingerprint scanners or sensors is hard to achieve. It appears that irrespective of the method employed, there will always be the need to establish a threshold or perhaps perform threshold analysis that will enforce details of candidate fingerprints to be consistent with fingerprints expected by the method under consideration.

2 Related Studies

In pattern recognition, the representation of patterns can be considered as feature extraction and is divided into four groups; statistical pixel features, algebraic features, visual features and transform coefficient features [13]. The following provide a short description of some of the related studies with respect to these techniques.

Mansukhani et al. [14] observed that, in order to compensate for the different orientations of two fingerprint images, matching systems should use a reference point and a set of transformation parameters. Due to this, fingerprint minutiae points were compared with their positions relative to the reference points using a set of thresholds for the various matching features. However, a pair of minutiae points might have similar values for some of the features which are compensated by dissimilar values for the others. Unfortunately, this trade-off cannot be modelled by arbitrary

thresholds since it might lead to a number of false matches. Instead, given a list of potential correspondences of minutiae points, static classifier such as a support vector machine (SVM) was used to eliminate some of the false matches. A 2-class model was further built using sets of minutiae correspondences from fingerprint pairs known to belong to the same or different users were used to reduce the number of false minutiae matches.

A fingerprint verification system based on a set of invariant moment features and a non-linear Back Propagation Neural Network (BPNN) verifier was proposed by Yang and Park [15] which was used to counter the demerits of the traditional minutiae based methods. The proposed system which contained an off-line stage for template processing and an on-line stage for testing was evolved. The pre-processed fingerprints helped in detecting a reliable and unique reference point to determine the Region-of-Interest (ROI). Features of the ROI were extracted using the proposed method and its performance compared with other methods based on absolute distance as a similarity measure. Their experimental results showed that the proposed method with BPNN matching had a higher matching accuracy, while the method with absolute distance had a faster matching speed.

In 2009, Khan et al. [16], as a result of high complexity required by the minutiae extraction algorithm, provided a new approach which uses wavelet based features, fused with minutiae based features for the purpose of matching. However, the result still yielded false minutiae points which served as a drawback to the proposed method. Although previous attempts were made to overcome this challenge by performing post-processing on the fingerprint image, it led to the elimination of some valid minutiae points which made them conclude that the strength of their matching algorithm depended highly on the strength of features extracted.

In the paper by Bhowmik et al. [17], a Euclidean distance based minutia matching algorithm was proposed to further improve the matching accuracy in fingerprint verification system. This was done by extracting the matched minutia pairs from both test and template datasets using the smallest minimum sum of closest Euclidean distance (SMSCED) corresponding with the rotation angle and chosen threshold values. The algorithm only used the minutia location instead of using the minutia type and orientation angle as in the traditional minutiae approach to reduce the effect of non-linear distortion. In this method it was evident that knowing and having a good threshold value resulted in a higher accuracy with improved verification and rejection rate.

In context, Elmir et al. [18] proposed an algorithm based on minutiae and singular points localization using Gabor filter on FVC2004 databases and FingerCell database. Based on the understanding of radial basis function, neural network and support vector machine they exploited the use of spike neural networks in order to develop codification and recognition algorithm. Performance Evaluation proved that, the spike neural network achieved a good recognition rate closer to rates achieved by other methods but in a very short time making its application useful.

A solution to this was proposed by Chengming et al. [19] where fingerprint matching was based on motion coherence which is useful for fingerprint feature matching with an improvement to performance. However, the performance of the automatic fingerprint identification system was significantly poor in situations where fingerprint images had poor qualities. One solution to Chengming et al. method as an enhancement algorithm was proposed by Zhang and Jing [20] using Gabor wavelets due to its ability to extract features in both spatial and spectral domain dynamically. The method as reported improved image quality significantly.

Qinghui and Xiangfei [21] also made a systematic elaboration on the correlation theories of fingerprint recognition technology with several essential algorithms. The study went further to prove the efficiency of combining the features of a fingerprint image in a pretreatment process. They took into consideration

the fingerprint image intensification which is based on the gradation standardization, directional diagram and filters. These parameters were also based on the partial smoothing threshold value during binarization which ended up improving the fingerprint recognition and verification.

Conti et al. [22] in their study discussed the use of set of relevant local characteristics such as the ridge endings and bifurcations for fingerprint classification and matching. The difficulty posed by this method was that unlike fingerprint matching, fingerprint classification is based on fingerprint global features such as the core and delta singularity points. Unfortunately, finding singularity points in all fingerprint images appeared not to be a trivial problem and hence making acquisition process complex especially with the arch class. They therefore proposed a pseudo singularity point algorithm which aids in the detection and extraction of all possible singularity point to be used in fingerprint classification and matching. But the issue of one minutia per each fingerprint query having multiple candidate matching minutiae in template fingerprint is profound in local structure matching. They indicated that, getting one-to-one matching pairs was difficult and therefore had great impact on performance of fingerprint matching algorithm.

A new approach for fingerprint verification based on wavelets and pseudo Zernike moment (PZM) was also proposed by Pokhriyal and Sushma [23] which is robust to noisy images, invariant to rotation and have a good image reconstruction capability. In their work, the PSM was used for global analysis and feature extraction. The Wavelets were also for local analysis and feature extraction from the fingerprint image and with this hybrid approach better verification rate was achieved. Unlike the conventional minutiae matching algorithms, Ackerman and Ostrovsky [6] in 2012 proposed an algorithm which takes into account region and line structures that exist between minutiae pairs and allows for more structural information of the fingerprint to be accounted for thus resulting in stronger certainty of matching minutiae. Evidence from this proposed method gives a stronger assurance that using such data could lead to faster and stronger matches.

3 Methodology

From the related studies it is quite evident that, quite a number of methods already exist for extracting unique features found in fingerprint image, each with its own advantages and disadvantages. For example there are widely used methods like Fast Fourier Transform (FFT) which may be used to perform this task. Unfortunately, according to [24], they do not provide enough degree of freedom in the so called signal cutting problem. This makes it less efficient to be used to analyze data that literary lives on curves or surfaces. And consequently, performs badly when used for irregular sampling of data. Due to the nature of Data and analysis required in this study, we required a method that is computationally fast and can reveal aspect of data like trends, breakdown points and discontinuities. Based on the assessment from the related studies, we chose wavelet transform due to its strength in the respective requirements as well as its dilation and translation properties which makes it multi-resolution analytic. We also considered the fact that when threshold values were chosen well, wavelets based methods performed much better than its peers. In the following sections, we discuss the how we feature vector for recognition was extracted and the corresponding and how the threshold analysis conducted.

3.1 Source and organization of dataset

The dataset used for this study was acquired from Fingerprint Verification Competition (FVC2004) [25] dataset, one of the most popular and standard databases for studies like this. Its content was created from 24 volunteers randomly partitioned into three groups of 30 persons with each group associated to a different fingerprint scanner. Each volunteer appeared in three distinct sessions, with

at least two weeks time separating each session. Each fore and middle finger of both hands (four fingers total) of each volunteer were scanned by interleaving the acquisition of the different fingers to maximize differences in finger placement. The sensor platens were not systematically cleaned and no attempts were made to control image quality. At each session, four impressions were acquired of each of the four fingers of each volunteer. To imitate real scenario, each person was asked in the first session to put the finger at a slightly different vertical position (producing impressions 1 and 2) and to alternate low and high pressure against the sensor surface (producing impressions 3 and 4). In the second session, each person was asked to exaggerate skin distortion (producing impressions 5 and 6) and rotation (producing impressions 7 and 8) of the finger. In the third session, fingers were dried (producing impressions 9 and 10) and finally moistened (producing impressions 11 and 12).

In total, 120 fingers with 12 impressions each were collected resulting in three separate datasets (DB1, DB2 and DB3). In this study, we used DB3 which contains 880 fingerprints in total created from 8 randomly selected impressions (figure 1) out of the 12 impressions per finger. The dataset was further divided into two groups of 800 and 80 respectively with the later serving as the set of candidate fingerprints.



Figure 1: Randomly selected fingerprints from the same person showing varying impressions.

3.2 Preprocessing and feature extraction

Fingerprint images acquired from FVC2004 [25] were initially preprocessed into its matrix representation and resized to a resolution of 256×256 since most wavelets we will construct works best on images with dimension in the powers of two, that is 2^n and in our use case, $n = 8$. In the following subsection we review briefly the process used for the feature extraction. This involves fast wavelet transform decomposition, estimation of local orientation and finally extraction of unique features from the dominant local orientation estimated.

3.2.1 Decomposition by fast wavelet transform:

The Fast Wavelet Transform (FWT) of the image say, x is calculated [26,27] by passing it through a series of filters. At the initial stage, the image is first passed through a low pass filter with impulse response g resulting in a convolution of the two as shown in Eqn (3.1)

$$y[n] = (x * g)[n] = \sum_{k=-\infty}^{\infty} x[k]g[n - k] \quad (3.1)$$

and finally passed through a high pass filter to decompose the signal simultaneously. The output of this process results in obtaining the detail coefficients from the high-pass filter and approximation coefficients from the low-pass filter. However, according to the Nyquist's rule, half the frequency of the original image has been removed after the process hence the need to discard the other half of

the frequencies. The filter outputs are then sub-sampled by 2 as follows:

$$y_{low}[n] = \sum_{k=-\infty}^{\infty} x[k]g[2n - k] \quad (3.2)$$

$$y_{high}[n] = \sum_{k=-\infty}^{\infty} x[k]h[2n - k] \quad (3.3)$$

Since only half of each filter output characterizes the signal, the decomposition reduces the time resolution by half. However, each output has half the frequency band of the input which causes the frequency resolution to double as shown in Figure 2. Using the sub-sampling operator \downarrow ,

$$(x \downarrow k)[n] = y[kn] \quad (3.4)$$

And to show the presence of convolution, Eqn's (3.2 and 3.3) can be written as:

$$y_{low} = (x * g) \downarrow 2 \quad (3.5)$$

$$y_{high} = (x * h) \downarrow 2 \quad (3.6)$$

However, computing a complete convolution xg with subsequent down-sampling increases the complexity of the computing time. These require an optimization technique where these two computations will be interleaved hence the need to apply the lifting scheme [26]. This decomposition is repeated to further increase the frequency resolution and the approximation coefficients decomposed with high and low pass filters and then down-sampled. The process is normally [28] represented as the binary tree with nodes representing the subspace with different time-frequency localization. The tree is known as a filter bank as shown in Figure: 3.

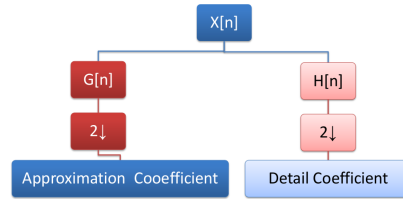


Figure 2: Block diagram of filter analysis

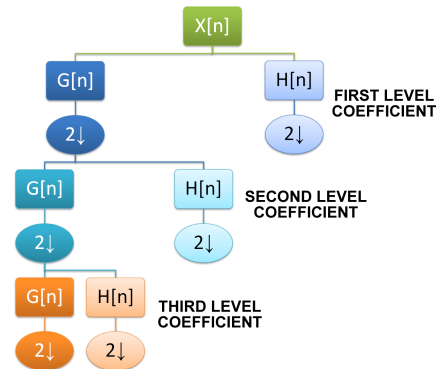


Figure 3: A three level filter bank

3.2.2 Estimation of Local Orientation

The approximation coefficients and the detail coefficients from the fast wavelet transform decomposition exposes the details of the fingerprint image for feature extraction. In particular, the local dominant orientation is efficiently calculated after the transformation. To estimate the local dominant orientation of the image, the following steps were carried out.

1. Magnitude of Image Gradient: The Sobel gradient G_{xy} in the x -direction G_{xy}^x and y -direction G_{xy}^y is applied to the image at each level and its magnitude computed for using Eqn. (3.7).

$$G_{xy} = (|G_{xy}^x| + |G_{xy}^y|) \quad (3.7)$$

2. Image Orientation: The resultant gradient of the image is then used to calculate the phase angle θ_{xy} of the image using Eqn. 3.8.

$$\theta_{xy} = \tan^{-1} \left(\frac{G_{xy}^y}{G_{xy}^x} \right) \quad (3.8)$$

3. Image Coherence: With Eqn. 3.7 and Eqn. 3.8, the image coherence δ_{xy} is determined with window size $N = 5$.

$$\delta_{xy} = \frac{\sum_{i=1}^N \sum_{j=1}^N G_{ij} \cos(\theta_{xy} - \theta_{ij})}{\sum_{i=1}^N \sum_{j=1}^N G_{ij}} \quad (3.9)$$

4. Local Dominant Orientation: Results from Eqn. (3.9) coupled with Eqn. (3.7) is used to estimate the dominant local orientation θ with window size $N = 8$

$$\theta = \frac{1}{2} \tan^{-1} \left(\frac{\sum_{i=1}^N \sum_{j=1}^N \delta_{ij}^2 \cos(2\theta_{ij})}{\sum_{i=1}^N \sum_{j=1}^N \delta_{ij}^2 \sin(2\theta_{ij})} \right) + \frac{\pi}{2} \quad (3.10)$$

3.2.3 Unique Feature Extraction

In order to extract unique features, the gray-level spatial dependence matrix (GLSPM) which generally allows one to examine the texture of an image by considering the spatial relationship of pixels is used [29,30]. The GLSPM characterizes the texture of an image by calculating how often pairs of pixel with specific values and in a specified spatial relationship occurs in the image, allowing extraction of various statistical measures from it. The local dominant orientation estimated is known to contain so many vital information, useful for fingerprint recognition and for the purpose of the study, the Energy, Contrast, Correlation and Homogeneity in the offsets of 0, 45, 90 and 135 were extracted as the unique features to represent a particular fingerprint. The energy (uniformity) or the angular second moment provides the sum of squared elements in the GLSPM. The contrast measures the local variations in the GLSPM. We note that the respective offsets were carefully chosen in order to achieve rotation invariance. The correlation also measures the joint probability occurrence of the specified pixel pairs and finally the homogeneity measures the closeness of the distribution of elements in the GLSPM to its diagonal. All the features including the threshold and the standard deviation extracted as edge parameters from each image at each level of decomposition are concatenated to form the fingerprint signature and stored in database for matching and recognition purposes. In order to identify the best threshold for recognition, this process is repeated using several families of wavelets tabulated in table 1. Note that a wavelet of type (x,y) means the wavelet has x vanishing moments for the

Table 1: List of Wavelet Families used in the performance analysis.

Code	Family Name	Type
BIOR	Biorthogonal Spline Wavelet	1.1,1.3,1.5,2.2,2.4,2.6,2.8,3.1,3.3,3.5,3.7,3.9,4.4,5.5,6.8
RBIO	Reverse Bi-orthogonal Spline Wavelet	1.1,1.3,1.5,2.2,2.4,2.6,2.8,3.1,3.3,3.5,3.7,3.9,4.4,5.5,6.8
SYMS	Symlets	2-8
COIF	Coiflets	1-5
DAUB	Daubechies	1-10
HAAR	Haar	

px decomposition wavelet and y vanishing moment for the reconstruction wavelet.

3.3 Fingerprint Recognition and Performance Analysis

In order to perform matching, the final feature vectors of the fingerprint to be recognized are first extracted and stored as fingerprint signature database. The candidate fingerprint image is then

processed and compared with the stored fingerprint signatures using the Euclidean Distance between the two features extracted. A Match (Accept) is achieved if the Euclidean distance between the two features is smaller than a predefined threshold otherwise rejected as a mismatch. The following performance indicators based on [6,25] were also used in order to analyse threshold values for the various families of wavelets employed in the study:

1. The probability that an unauthorized person is incorrectly accepted as authorized person. This is estimated by using Match Count (MC) per the impostor attempts, known as False Acceptance Rate (FAR).
2. The second indicator is the probability that an authorized person is wrongfully considered as an unauthorized person calculated as number of Miss Match Count (MMC) per the genuine attempts. This is called the False Rejection Rate (FRR).
3. The third indicator measures the rate at which match occurs successfully known as the Total Success Rate (TSR)
4. The last indicator is the Equal Error Rate (ERR) and it is the rate at which both accept and reject rates are equal.

4 Results and Analysis of Fingerprint Recognition

In this work, the organization of the total extracted features was categorized into three main groups based on the level of resolution. Hence, each level contains exactly 108 tuple feature vector and since a three level resolution was applied to the fingerprint image, each fingerprint signature will be a total of $3 \times 108 = 324$ tuple vector. Because the dataset used for the study was built for the purpose of competition using worse case scenarios, even images that were known to be different showed visually no significant difference.

For example in Figures (4a and 4b) when we plotted three feature vectors extracted from two fingerprint images from the same person and the last fingerprint image from a completely different person, there was visually no significant difference between the three images at the three levels of decomposition. In particular the red and blue plots represent feature vectors from the same fingerprint image while the black represents fingerprint image belonging to a different person. We note that the significantly

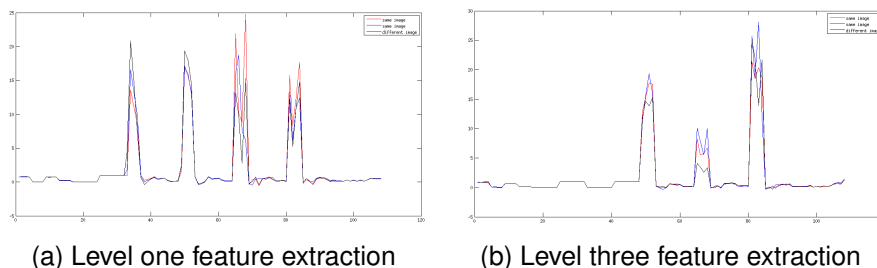


Figure 4: Graph of feature vectors extracted at various levels of decomposition using reverse bi-orthogonal wavelet of type 3.1

closer values allowed us to test for sensitivity of the predetermined threshold values and accuracy of the matching algorithm. Due to the multiple impression and deliberate noise found in the dataset, the similarity function (based on Euclidean transform) used in this study for recognition of an authorized person was applied to candidate signatures and the stored signatures at all three levels of decomposition based on a predefined threshold.

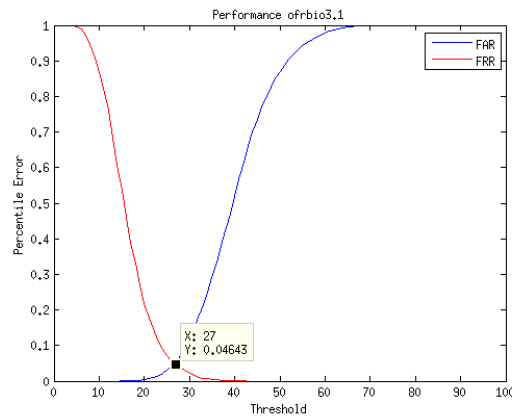
4.1 Analysis of predefined threshold

Threshold as it stands in fingerprint recognition plays an important role and this is a predefined value used in determining whether a particular fingerprint (or candidate fingerprint) matches any known fingerprint in the template database. This decision is based on calculating the Euclidean distance or transform between the candidate fingerprint and the template database. When the distance value is less than a predefined threshold, the candidate fingerprint will be counted as a match. This helps in evaluating the FAR and FRR values. Generally the threshold values ranges from 0 to 100. In order to establish good threshold values for each mother wavelet used in the study, we analysed several threshold values ranging from 0 to 100. The value at which the percentage of false acceptance rate equals the false rejection rate is determined as the percentage of equal error rate. The threshold at which the equal error rate is found is considered as the best threshold for that particular method.

It appears that the threshold value must be relatively small to have a good recognition or performance rate. The performance parameters such as FAR, FRR and TSR for the various mother wavelets employed were computed based on the extracted feature vectors. Table 2a shows variations of FAR and FRR using the various pre-defined threshold values.

Table 2: Analysis of threshold values using bi-orthogonal wavelet of type 3.1

Threshold	%FAR	%FRR	%TSR
12	0	76.25	23.75
15	0.02	53.75	46.25
18	0.10	33.21	66.79
21	0.63	17.64	82.36
24	2.06	9.00	91.00
27	5.13	4.64	95.36
30	11.68	2.32	97.68
33	21.47	0.86	99.14
36	33.47	0.39	99.61
39	47.07	0.11	99.89
45	73.66	0	100.00
48	82.48	0	100.00



(a) Results for FAR, FRR and TSR for sample threshold values

(b) A graphical representation of FAR and FRR values

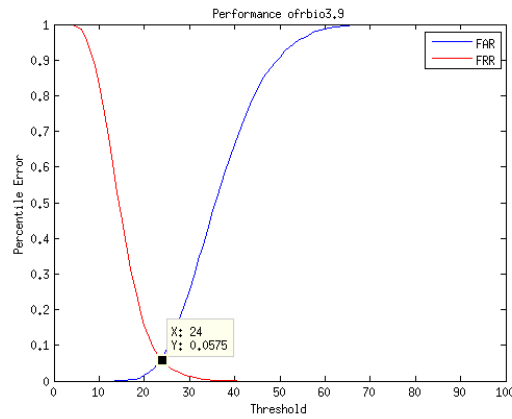
The respective graph is shown in Figure 2b with the EER (Percentile error) value in the vertical axis and the threshold value in horizontal axis. Particularly, table 2a shows the computed results for reverse bi-orthogonal type 3.1 wavelet. We observed that the FAR increases whiles the FRR decreases as the threshold value increases which conforms to the general interpretation of type 1 and 2 errors.

Numerically, EER value obtained for the reverse bi-orthogonal type 3.1 mother wavelet was 0.04643 or 4.64% and this happens at a threshold value of 27 with total success rate (TSR) of 95.36%. Tables (3 and 4) also demonstrate the effect of threshold values on different wavelet families. In particular we show the results for bi-orthogonal wavelet of type 3.9 and 4.4 which performed quite well on the dataset we used for the analysis.

In using the reverse bi-orthogonal type 3.9 wavelet, an EER value of 0.0575(5.75%) was found (Figure 3b and Table 3a) and this occurred at a threshold value of 24 with total success rate of 94.25%.

Table 3: Threshold analysis for reverse bi-orthogonal wavelets of type 3.9

Threshold	%FAR	%FRR	%TSR
12	0	68.61	31.39
15	0.02	45.07	54.94
18	0.53	25.54	74.46
21	2.34	12.11	87.89
24	6.73	5.75	94.25
27	14.81	2.64	97.36
30	25.47	1.32	98.68
33	38.08	0.54	99.32
36	51.23	0.18	99.82
39	62.95	0.04	99.96
42	73.13	0	100.00
45	81.92	0	100.00
48	87.86	0	100.00



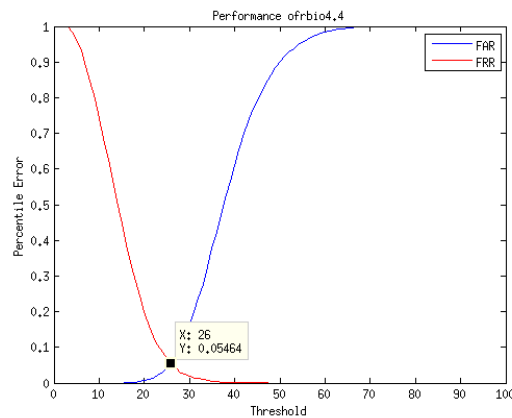
(a) FAR, FRR and TSR for various threshold values using the reverse bi-orthogonal wavelet 3.9

(b) A graph of variation of FAR and FRR using bi-orthogonal type 3.9 wavelet

Again, in the application of the reverse bi-orthogonal type 4.4 mother wavelet, an EER value of 0.05464 (5.46%) was achieved at a threshold value of 26 as illustrated in Figure: 4b with a total success rate of 94.54% as shown in table 4a.

Table 4: Analysis of threshold values for reverse bi-orthogonal wavelet 4.4

Threshold	% FAR	% FRR	% TSR
12	0	62.68	37.32
15	0	44.64	55.36
18	0.20	28.54	71.46
21	1.05	16.04	83.96
24	3.11	8.71	91.29
27	5.58	5.46	94.54
30	16.46	1.96	98.04
33	27.76	1.00	99.00
36	42.24	0.46	99.54
39	56.46	0.18	99.82
42	69.92	0.11	99.89
45	79.35	0.04	99.96
48	86.48	0	100.00



(a) FAR, FRR and TSR for various threshold values using the reverse bi-orthogonal type 4.4 wavelet

(b) Graphical representation of FAR and FRR Values

In order to test the sensitivity of the threshold values, 53 wavelets families with closely related properties and strength were studied. Table 5 gives a summary of all the wavelet families used in this study ordered according to EER values.

Table 5: Summary of families of mother wavelet used with their corresponding EER Values

Wavelet	Threshold	EER	%EER	Wavelet	Threshold	EER	% EER
RBIO3.1	27.00	0.04630	4.64	DB2	23.83	0.07285	7.29
RBIO4.4	26.00	0.05464	5.46	RBIO5.5	26.00	0.07286	7.29
RBIO3.9	24.00	0.05750	5.75	COIF2	23.90	0.07324	7.32
BIO3.1	21.00	0.05812	5.81	BIOR1.3	24.42	0.07331	7.33
SYM4	24.56	0.06104	6.10	SYM5	23.34	0.07285	7.41
RBIO2.4	22.38	0.06187	6.19	BIOR2.2	25.14	0.07446	7.45
RBIO2.2	23.34	0.06222	6.22	SYM2	23.73	0.07510	7.51
DB6	23.88	0.06442	6.44	BIOR1.5	24.81	0.07541	7.54
BIO3.5	25.18	0.06460	6.46	DB7	23.78	0.07543	7.54
RBIO3.5	23.00	0.06500	6.50	SYM6	24	0.07561	7.56
DB5	24.00	0.06536	6.54	DB4	23.44	0.07607	7.61
BIOR2.6	25.81	0.06595	6.60	RBIO1.3	22.39	0.07677	7.68
BIOR5.5	19.19	0.06600	6.60	BIOR2.8	24.91	0.07688	7.69
BIOR3.9	25.38	0.06605	6.61	RBIO1.1	23.2	0.07778	7.78
DB9	23.75	0.06631	6.63	SYM3	24.34	0.07785	7.79
RBIO2.6	24.04	0.06656	6.66	SYM8	28	0.07786	7.79
BIOR3.3	23.87	0.06706	6.71	DB3	23.34	0.07789	7.79
RBIO3.7	24.00	0.06714	6.71	COIF3	23.61	0.07874	7.87
DB10	24.66	0.06744	6.74	DB8	23.36	0.07923	7.92
COIF1	24.00	0.06893	6.89	HAAR	23.11	0.07966	7.97
RBIO2.8	22.47	0.06994	6.99	RBIO1.5	22.16	0.08045	8.05
SYM7	23.00	0.07047	7.05	DB1	23	0.08214	8.12
COIF5	25.05	0.07111	7.11	BIOR4.4	22.07	0.08222	8.22
BIOR3.7	24.14	0.07163	7.16	BIOR6.8	23.62	0.08333	8.33
BIOR2.4	25.25	0.07181	7.18	BIOR1.1	22.93	0.08338	8.34
RBIO6.8	25.00	0.07250	7.25	RBIO3.3	24	0.08357	8.36
COIF4	24.72	0.07261	7.26				

5 Conclusions

In this paper, we have demonstrated the effect of using predefined threshold value during feature extraction, in an attempt to establish Equal Error Rate for fingerprint recognition on multiple impression dataset. Although most wavelets based feature extraction methods generally assumes traits that can efficiently extract fingerprint features for multiple impression datasets, the analysis conducted in this study indicates that predefined threshold values arbitrarily chosen during feature extraction have significant effect on what feature extraction method to chose and subsequently the recognition rate. Based on the dataset used in the study, the results showed that, among the studied wavelet methods used for feature extraction, the reverse biorthogonal wavelets assumed the least equal error rate and the highest recognition rate only at a specific threshold value and performed quite poorly otherwise The Analysis performed shows that a badly predefined threshold value can cause a rather

good feature extraction method to perform quite badly especially when the dataset contains multiple impressions not specifically known to the algorithm. The study has also shown that it is advisable to perform threshold analysis on datasets in order to obtain threshold values that can ensure high performance rate especially when comparing different methods or deciding on what method to adopt for feature extraction on multiple impression dataset.

Acknowledgment

We will like to acknowledge the support received from the National Institute for Mathematical Sciences, Ghana for this study.

Competing Interests

The authors declare that no competing interests exist.

References

- [1] Drahansky M. Fingerprint recognition technology - related topics. LAP, ISBN 978-3-8443-3007-6. 2011;172.
- [2] Medina-Perez MA, Garcia-Borroto M, Gutierrez-Rodriguez EA, Altamirano-Robles L. Improving fingerprint verification using minutiae triplets. *Sensors*. 2012;3418-3437.
- [3] Parziale G, Niel A. A fingerprint matching using minutiae triangulation. Proceedings of the 1st International Conference on Biometric Authentication, Hong Kong, China LNCS 3072. 2004;241-248.
- [4] Prabhakar S, Pankanti SH, Jain AK. Biometric recognition: Security and privacy concerns. *IEEE Security and Privacy*. 2003;33-42.
- [5] Tico M, Kuosmanen P. Fingerprint matching using an orientation-based minutia descriptor. *IEEE Trans. Pattern. Anal. Mach. Intell.* 2003;25:1009-1014.
- [6] Ackerman A, Ostrovsky R. Fingerprint recognition. Master's thesis, UCLA Computer Science Department; 2012.
- [7] Edward Hueske. Firearms and Fingerprints. Facts on File/Infobase Publishing; 2009.
- [8] Qi J, Yang S, Wang Y. Fingerprint matching combining the global orientation field with minutia. *Pattern Recogn. Lett.* 2005;26:2424-2430.
- [9] Dechman HG. Fingerprint identification standards for emerging applications. Technical report; 2012.
- [10] Ashbaugh David R. Ridgeology, modern evaluative friction ridge identification. Technical report, Forensic Identification Support Section, Royal Canadian Mounted Police; 1999.
- [11] Wang W, Li J, Chen W. Fingerprint minutiae matching based on coordinate system bank and global optimum alignment. In Proceedings of the 18th International Conference on Pattern Recognition, Hong Kong, China. 2006;4:401-404.

- [12] Dolezel M, Drahansky M, Urbanek J, Brezinova E, Kim T. Influence of skin diseases on fingerprint quality and recognition, new trends and developments in biometrics. Technical report, ISBN: 978-953-51-0859-7, In Tech. DOI: 10.5772/51992, 2012.
- [13] Hong Z. Algebraic feature extraction of image for recognition. *Pattern Recognition*. 1991;24:211-219.
- [14] Mansukhani P, Tulyakov S, Govindaraju V. Using support vector machines to eliminate false minutiae matches during fingerprint verification. In *SPIE Defense and Security Symposium (DSS)*, Orlando, FL, USA; 2007.
- [15] Yang JC, Park DS. Fingerprint verification based on invariant moment features and nonlinear bpnn. *International Journal of Control, Automation and Systems*. 2008;6(6):800-808.
- [16] Khan UM, Khan SA, Rehman RU. A fingerprint verification system using minutiae and wavelet based features. In *International Conference on Emerging Technologies*; 2009.
- [17] Bhowmik UK, Ashrafi A, Adham RRI. A fingerprint verification algorithm using the smallest minimum sum of closest euclidean distance. *International Conference on Electrical, Communications and Computers*. 2009;90-95.
- [18] Elmir Y, Elberrichi Z, Adjoudj R, Benyettou M. Personal identification by fingerprints based on gabor filters. In *Conference sur Informatique*; 2009.
- [19] Chengming W, Tiande G, Wang S. Fingerprint feature-point matching based on motion coherence. *Second International Conference on Future Information Technology and Management Engineering*. 2009;226-229.
- [20] Zhang Y, Jing X. Spectral analysis based fingerprint image enhancement algorithm. In *IEEE ASSP Magazine*; 2010.
- [21] Qinghui Z, Xiangfei Z. Research of key algorithm in the technology of fingerprint identification. *Second International Conference on Computer Modeling and Simulation*. 2010;282-184.
- [22] Conti V, Militello C, Vitabile S, Sorbello F. Introducing pseudo singularity points for efficient fingerprints classification and recognition. *International Conference on Complex, Intelligent and Software Intensive Systems*. 2010;10:368-375.
- [23] Pokhriyal A, Sushma L. A new method of fingerprint authentication using 2d wavelet. *Journal of Theoretical and Applied Information Technology*. 2010;13(2):131-138.
- [24] Sifuzzaman M, Islam MR, Ali MZ. Application of wavelet transform and its advantages compared to fourier transform. *Journal of Physical Sciences*. 2009;13:121-134.
- [25] Maltoni D, Maio D, Jain AK, Prabhakar S. *Handbook of Fingerprint Recognition*. Springer, London; 2009.
- [26] Goh SS, Jiang Q, Xia T. Construction of biorthogonal multiwavelets using the lifting scheme. *Applied and Computational Harmonic Analysis*. 2000;9(3):336-352.
- [27] Stephane Mallat. *A wavelet tour of signal processing: the sparse way*. Academic press; 2008.
- [28] Gonzalo Navarro. Wavelet trees for all. *Journal of Discrete Algorithms, 23rd Annual Symposium on Combinatorial Pattern Matching*. 2014;25:2-20.

- [29] Alaa Eleyan and Hasan Demirel. Co-occurrence matrix and its statistical features as a new approach for face recognition. Turkish Journal of Electrical Engineering & Computer Sciences. 2011;19(1):97-107.
- [30] Dinstein I, Haralick RM, Shanmugam K. Textural features for image classification. IEEE Transactions on Systems, Man, and Cybernetics. 1973;3(6):610-621.

©2015 Amoako-Yirenkyi et al.; This is an Open Access article distributed under the terms of the Creative Commons Attribution License <http://creativecommons.org/licenses/by/4.0>, which permits unrestricted use, distribution, and reproduction in any medium, provided the original work is properly cited.

Peer-review history:

The peer review history for this paper can be accessed here (Please copy paste the total link in your browser address bar)

www.sciencedomain.org/review-history.php?iid=727&id=6&aid=6883